

Synthesis and transition metal coordination chemistry of a novel hexadentate bispidine ligand

Peter Comba, Henning Rudolf and Hubert Wadepohl*

Universität Heidelberg, Anorganisch-Chemisches Institut, INF 270,
D-69120 Heidelberg, Germany

Electronic Supporting Information

Correspondence:

e-mail: peter.comba@aci.uni-heidelberg.de

Fax: +49-6221-546617

Table S1. Redox potentials of copper-bispidine complexes used for the correlation of with Cu^{II} complex stabilities in Figure S1 (references refer to the main text).^{4, 28-30, 32}

Ligand ^a	E(Cu ^{I/II}) [mV] (MeCN vs. Fc)	logK(Cu ^{II})
L ¹	-598	16.56(5)
Me ₂ -L ¹	-270	9.60(7)
L ²	-776	18.31(12)
L ^{2'}	-661	15.66(3)
L ³	-745	16.28(10)
L	-651	16.0
L ^{OH}	-671	16.3

^a abbreviations: see Figure S1 and Chart 1 in the manuscript

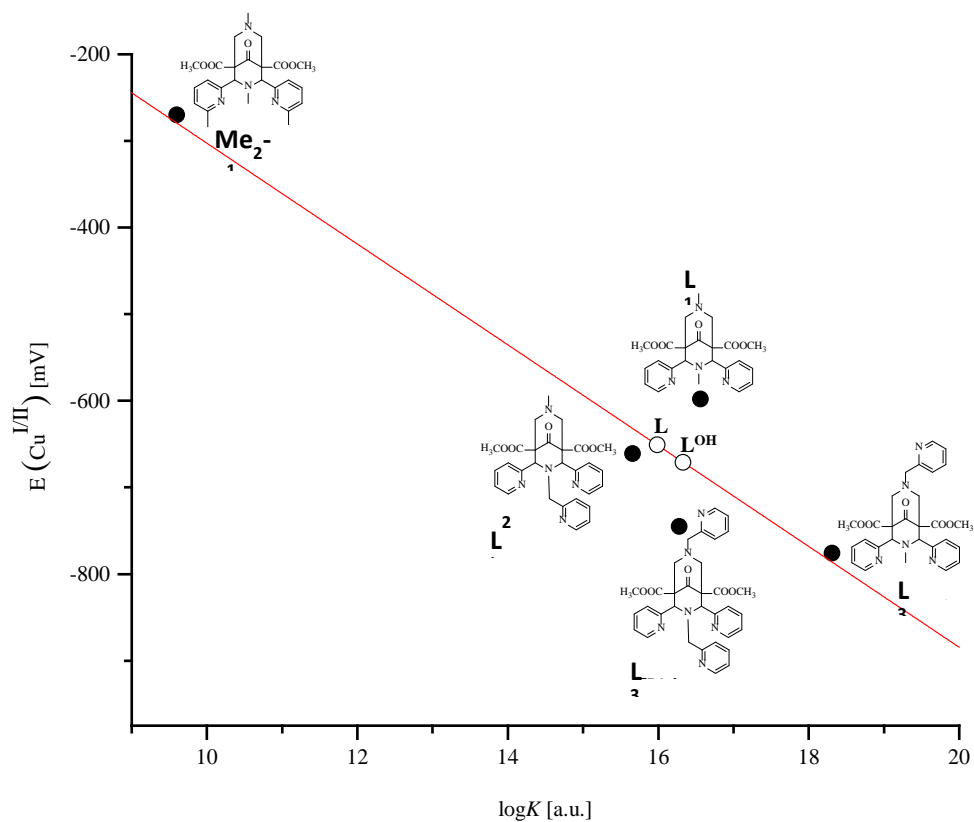


Figure S1. Plot of the redox potentials as a function of the Cu^{II} complex stability for the determination of the stability constants of ligands L and L^{OH} (data from Table S1).^{4, 28-30, 32}

Table S2. Structural analysis of the manganese complex (see Table 5 and Figure 4); best plane for the pentagonal bipyramidal structure (distances in Å):

molecule	1	2
RMSD (plane)	0.376	0.378
distance from plane		
N3	0.572(1)	0.574(1)
py1	-0.492(1)	-0.354(1)
py2	-0.347(1)	-0.470(1)
py3	0.060(1)	0.054(1)
py4	0.186(1)	0.194(1)

Table S3. Details of the crystal structure determinations of $[\text{Cu}^{\text{II}}(\text{L})]^{2+}$, $[\text{Cu}^{\text{II}}(\text{L}^{\text{OH}})]^{2+}$, $[\text{Fe}^{\text{II}}(\text{L})\text{OHMe}]^{2+}$, $[\text{Fe}^{\text{III}}(\text{L})\text{OMe}]^{2+}$, $[\text{Fe}^{\text{II}}(\text{L}^{\text{OH}})\text{Cl}]^+$, and $[\text{Mn}^{\text{II}}(\text{L})\text{Cl}]^+$

	$[\text{Cu}^{\text{II}}(\text{L})](\text{BF}_4)_2$	$[\text{Cu}^{\text{II}}(\text{L}^{\text{OH}})](\text{BF}_4)_2 \cdot 2\text{H}_2\text{O}$	$[\text{Fe}^{\text{II}}(\text{L})\text{OHMe}](\text{BF}_4)_2 \cdot \text{OEt}_2$	$[\text{Fe}^{\text{III}}(\text{L})\text{OMe}](\text{ClO}_4)_2 \cdot \text{H}_2\text{O} \cdot \text{NCMe}$	$[\text{Fe}^{\text{II}}(\text{L}^{\text{OH}})\text{Cl}]\text{Cl} \cdot \text{solv}$	$2[\text{Mn}^{\text{II}}(\text{L})\text{Cl}][\text{MnCl}_4] \cdot \text{MeO} \cdot \text{solv}$
formula	$\text{C}_{33.57}\text{H}_{34.13}\text{B}_2\text{CuF}_8\text{N}_6\text{O}_6$	$\text{C}_{33}\text{H}_{38}\text{B}_2\text{CuF}_8\text{N}_6\text{O}_7$	$\text{C}_{38.7}\text{H}_{48.7}\text{B}_2\text{F}_8\text{FeN}_6\text{O}_{7.7}$	$\text{C}_{36}\text{H}_{42}\text{Cl}_2\text{FeN}_7\text{O}_{16}$	$\text{C}_{33}\text{H}_{34}\text{Cl}_2\text{FeN}_6\text{O}_5$	$\text{C}_{34.5}\text{H}_{38}\text{Cl}_3\text{Mn}_{1.5}\text{N}_6\text{O}_{6.5}$
M_r	854.75	867.85	950.18	955.51	720.38	829.47
crystal system	monoclinic	monoclinic	monoclinic	triclinic	triclinic	monoclinic
space group	$P 2_1/c$	$P 2_1/c$	$P 2_1/n$	$P -1$	$P -1$	$P2_1/a$
$a / \text{\AA}$	20.74985(19)	20.7553(3)	10.538(5)	13.353(6)	8.40726(19)	20.546(2)
$b / \text{\AA}$	10.42825(8)	10.30900(12)	15.040(7)	13.488(6)	14.6959(3)	15.8473(17)
$c / \text{\AA}$	17.69608(16)	17.8036(2)	27.068(14)	13.681(6)	15.2169(4)	23.647(2)
$\alpha / ^\circ$				61.283(7)	79.632(2)	
$\beta / ^\circ$	102.4417(9)	103.2779(13)	99.311(8)	69.065(14)	84.430(2)	104.361(12)
$\gamma / ^\circ$				68.674(11)	76.8063(18)	
$V / \text{\AA}^3$	3739.23(6)	3707.55(8)	4233(3)	1962.1(15)	1797.48(8)	7458.9(14)
Z	4	4	4	2	2	8
F_{000}	1746	1780	1969	990	747	3492
$d_c / \text{Mg} \cdot \text{m}^{-3}$	1.518	1.555	1.491	1.617	1.331	1.477
X-radiation, $\lambda / \text{\AA}$	Cu- $K\alpha$, 1.5418	Mo- $K\alpha$, 0.71073	Mo- $K\alpha$, 0.71073	Mo- $K\alpha$, 0.71073	Mo- $K\alpha$, 0.71073	Mo- $K\alpha$, 0.71073
μ / mm^{-1}	1.652	0.685	1.491	0.606	0.613	0.784
max., min. transmission factors	0.957, 0.785	0.965, 0.912	0.7462, 0.6976	0.7464, 0.7022	1.0000, 0.7692	0.898, 0.587
data collect. temperat. /K	110(1)	110(1)	100(2)	100(2)	110(1)	200(2)
θ range / $^\circ$	4.8 to 70.8	3.2 to 25.7	1.5 to 31.0	1.7 to 32.5	3.3 to 29.9	2.6 to 30.5
index ranges (indep. set) h,k,l	-25 ... 25, -12 ... 12, -	-25 ... 25, -12 ... 12, -	-15 ... 15, -21 ... 21, -	-19 ... 20, -20 ... 20, -	-11 ... 11, -20 ... 20, -	-29 ... 29, -22 ... 22, -

	$[\text{Cu}^{\text{II}}(\text{L})](\text{BF}_4)_2$	$[\text{Cu}^{\text{II}}(\text{L}^{\text{OH}})](\text{BF}_4)_2 \cdot 2\text{H}_2\text{O}$	$[\text{Fe}^{\text{II}}(\text{L})\text{OHMe}](\text{BF}_4)_2 \cdot \text{OEt}_2$	$[\text{Fe}^{\text{III}}(\text{L})\text{OMe}](\text{ClO}_4)_2 \cdot \text{H}_2\text{O} \cdot \text{NCMe}$	$[\text{Fe}^{\text{II}}(\text{L}^{\text{OH}})\text{Cl}]\text{Cl} \cdot \text{solv}$	$2[\text{Mn}^{\text{II}}(\text{L})\text{Cl}][\text{MnCl}_4] \cdot \text{MeO} \cdot \text{solv}$
	21 ... 21	21 ... 21	39 ... 39	20 ... 20	21 ... 21	33 ... 32
reflections measured	92804	70356	103429	50130	97442	88584
unique $[R_{\text{int}}]$	7169 [0.0403]	7025 [0.0649]	13502 [0.0516]	13127 [0.0449]	9872 [0.0727]	22313 [0.0947]
observed $[I \geq 2\sigma(I)]$	6735	5859	10336	10051	8736	11153
parameters refined	528	524	613	571	449	940
GooF on F^2	1.050	1.042	1.043	1.033	1.210	0.795
R indices $[F > 4\sigma(F)]$ $R(F)$, $wR(F^2)$	0.0803, 0.2317	0.0434, 0.0991	0.0589, 0.1608	0.0429, 0.1030	0.0659, 0.1307	0.0473, 0.1073
R indices (all data) $R(F)$, $wR(F^2)$	0.0830, 0.2343	0.0556, 0.1055	0.0809, 0.1757	0.0646, 0.1152	0.0775, 0.1346	0.1034, 0.1190
Difference density: max, min /e $\cdot\text{\AA}^{-3}$	2.137, -1.166	0.908, -0.773	1.504, -0.788	0.893, -0.688	0.486, -0.503	1.51, -0.99

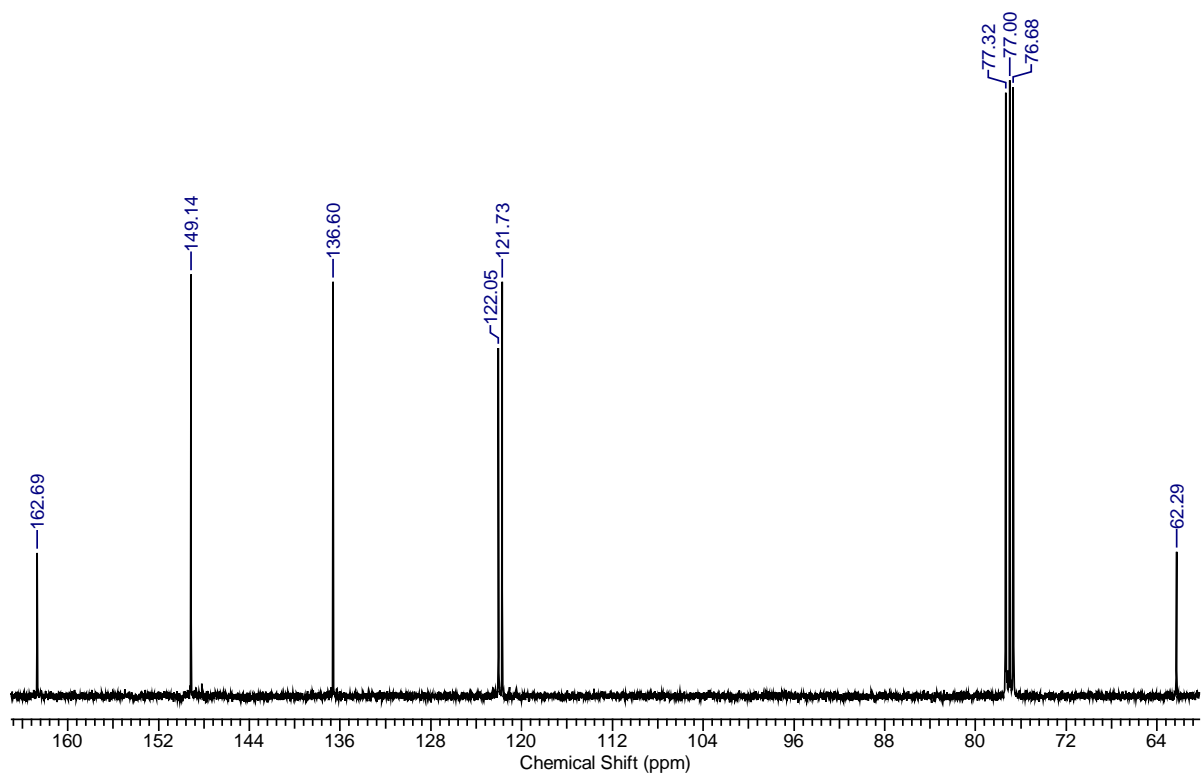
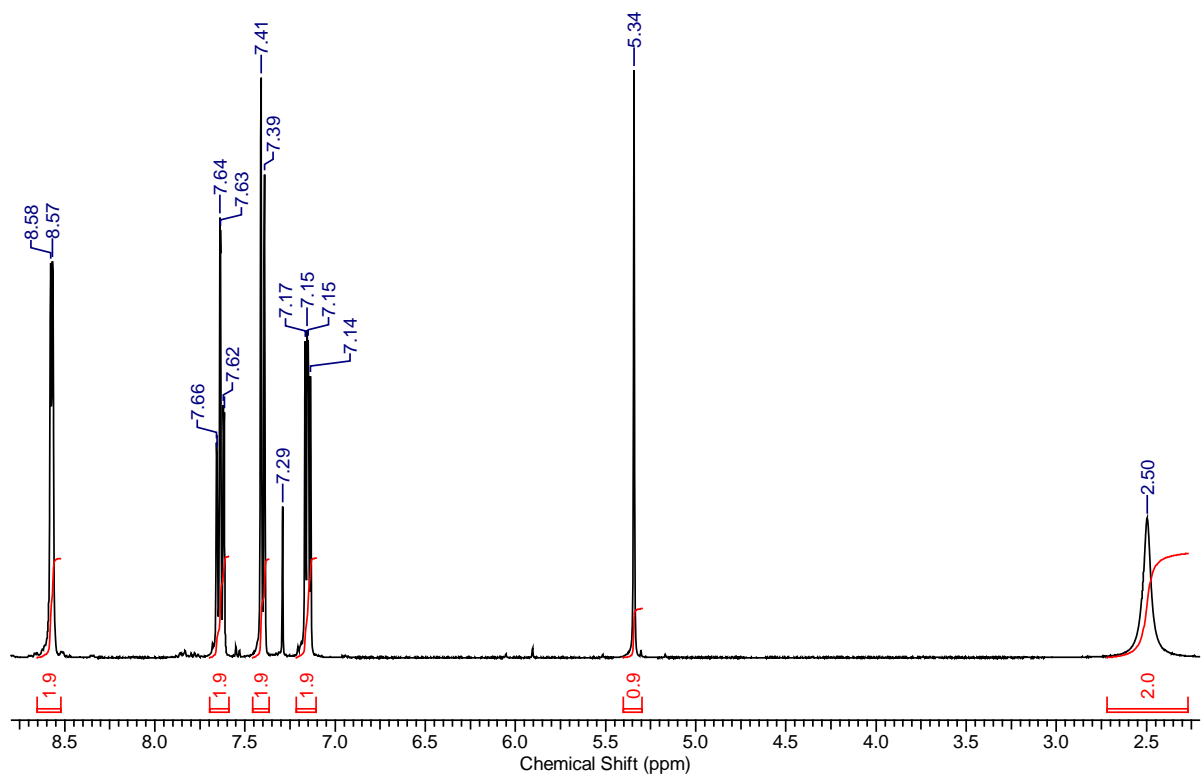


Figure S2: NMR Spectra of Di(2-pyridyl)methylamine

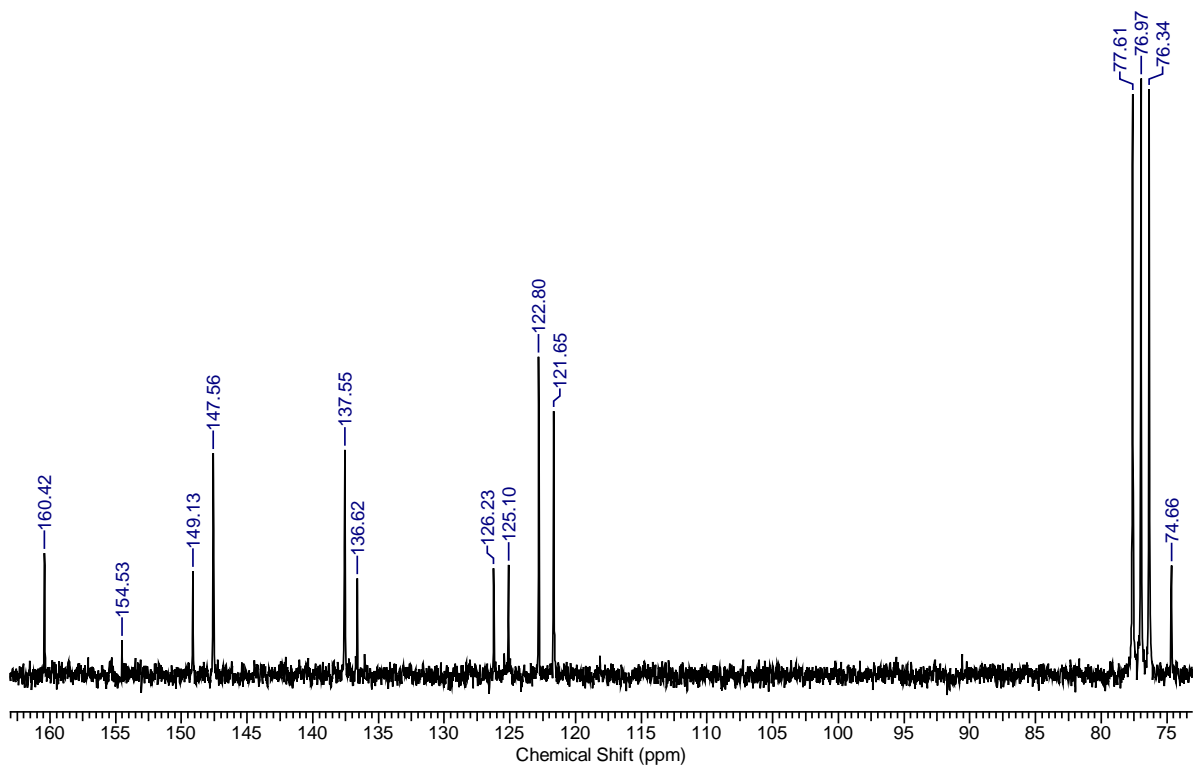
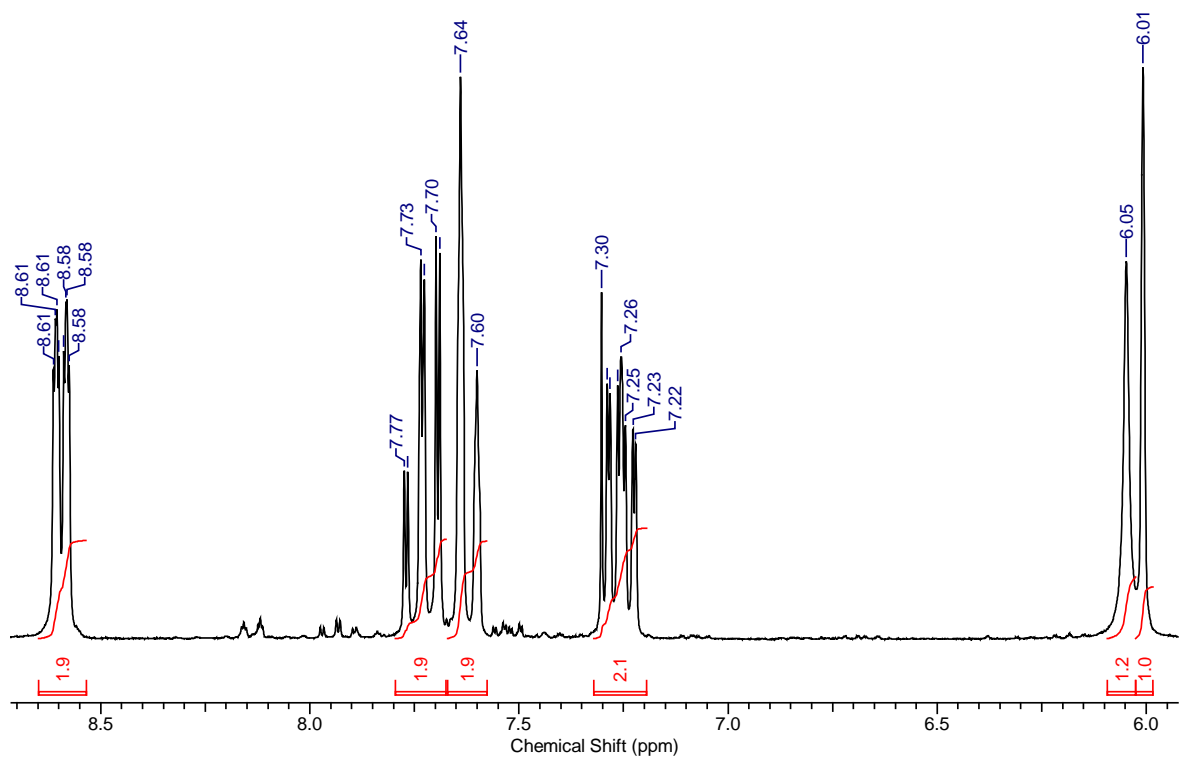


Figure S3: NMR Spectra of Di(2-pyridyl)methanol

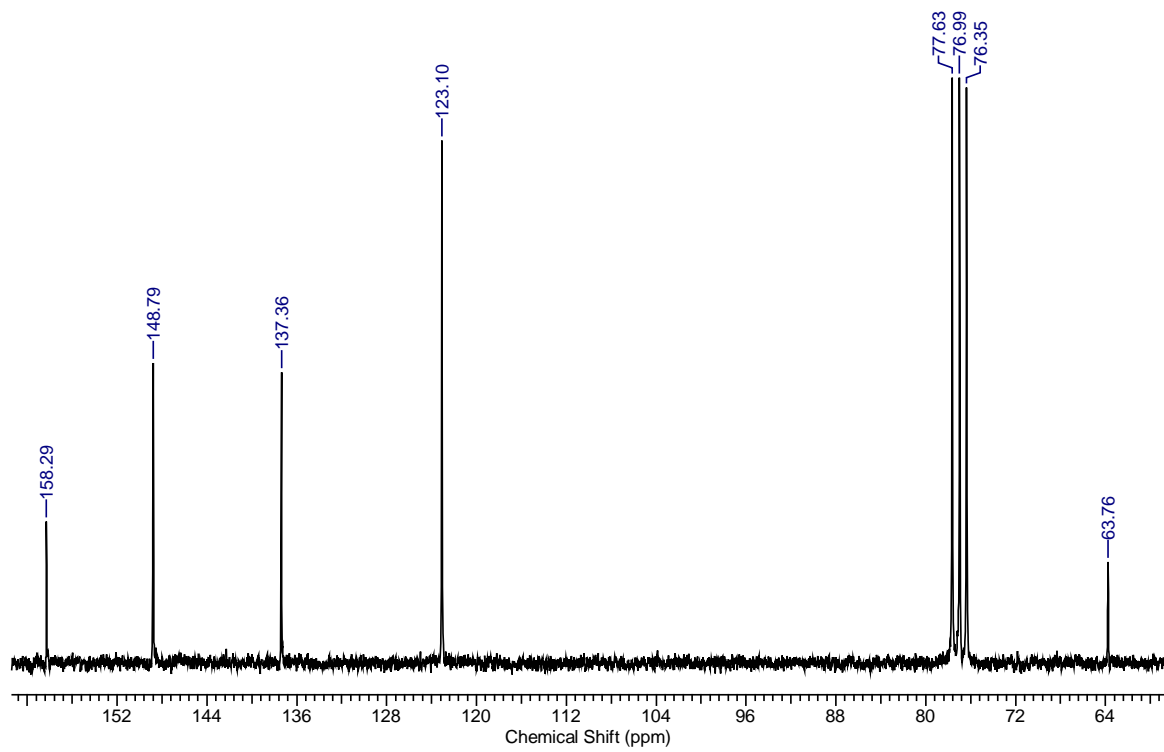
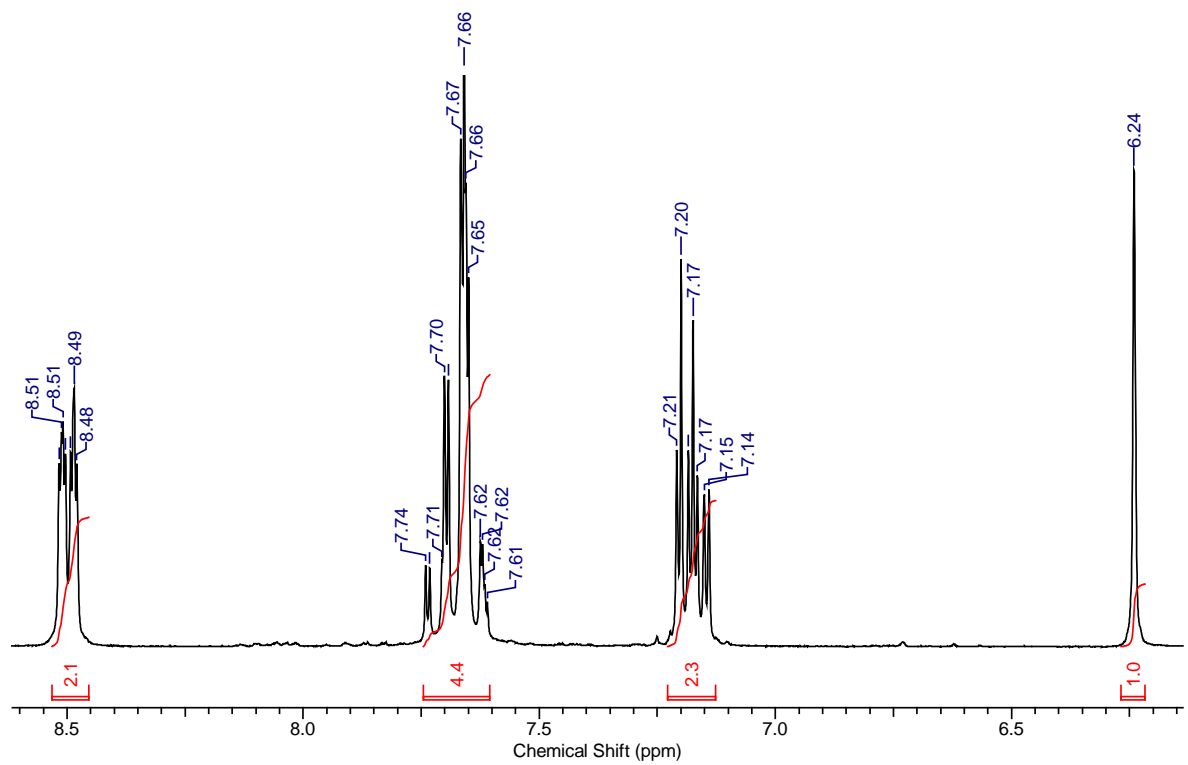


Figure S4: NMR Spectra of Di(2-pyridyl)methylchloride

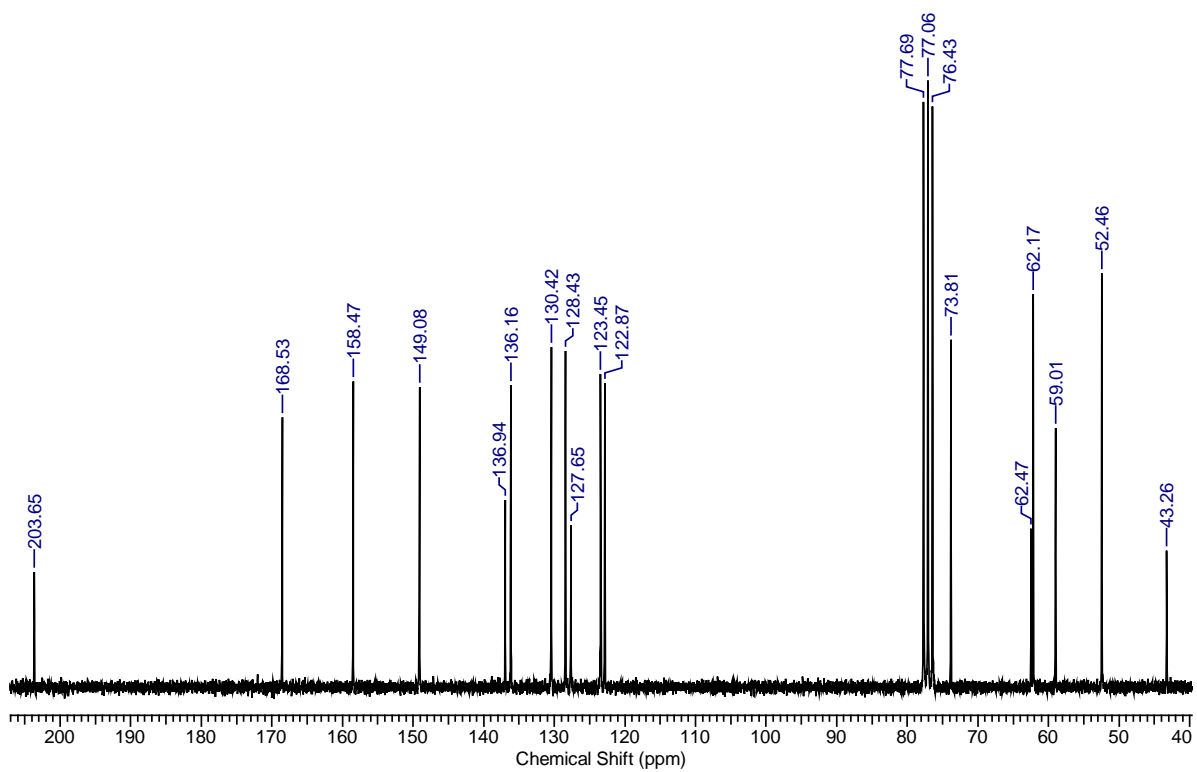
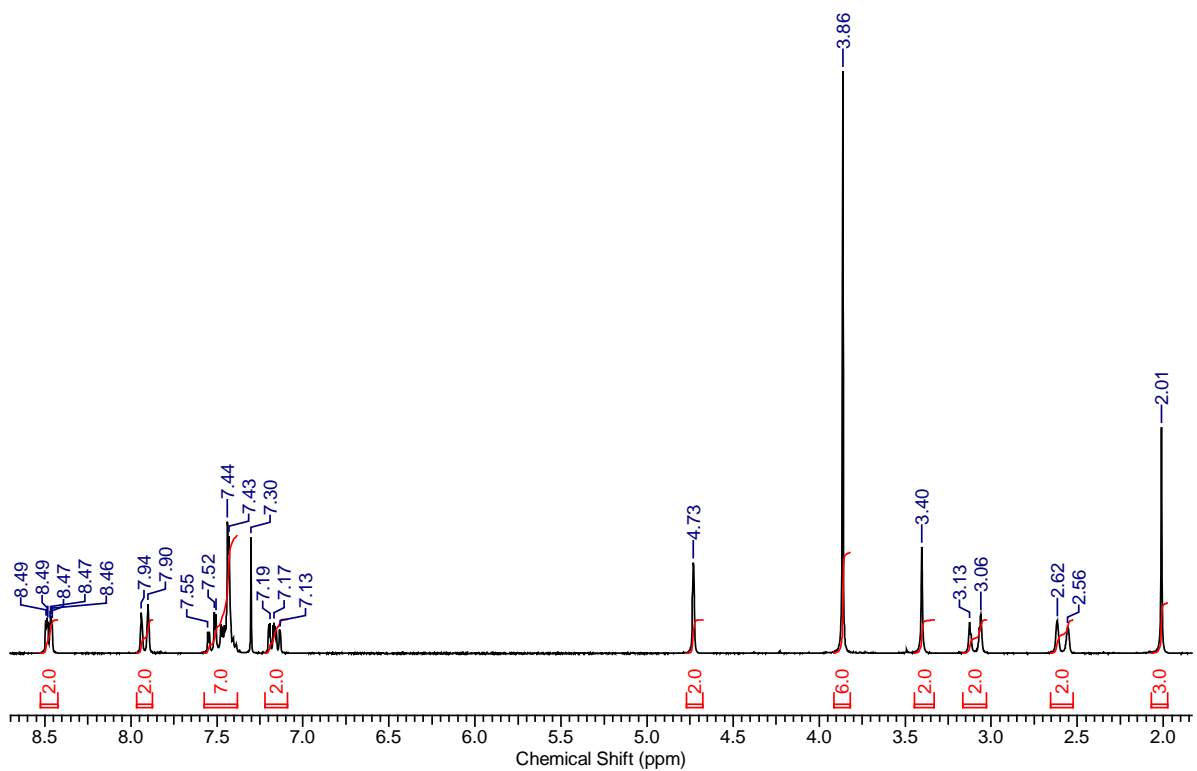


Figure S5: NMR Spectra of Dimethyl-(7-benzyl-3-methyl-9-oxo-2,4-bis(2-pyridyl)-3,7-diazabicyclo[3.3.1]nonane)-1,5-dicarboxylate

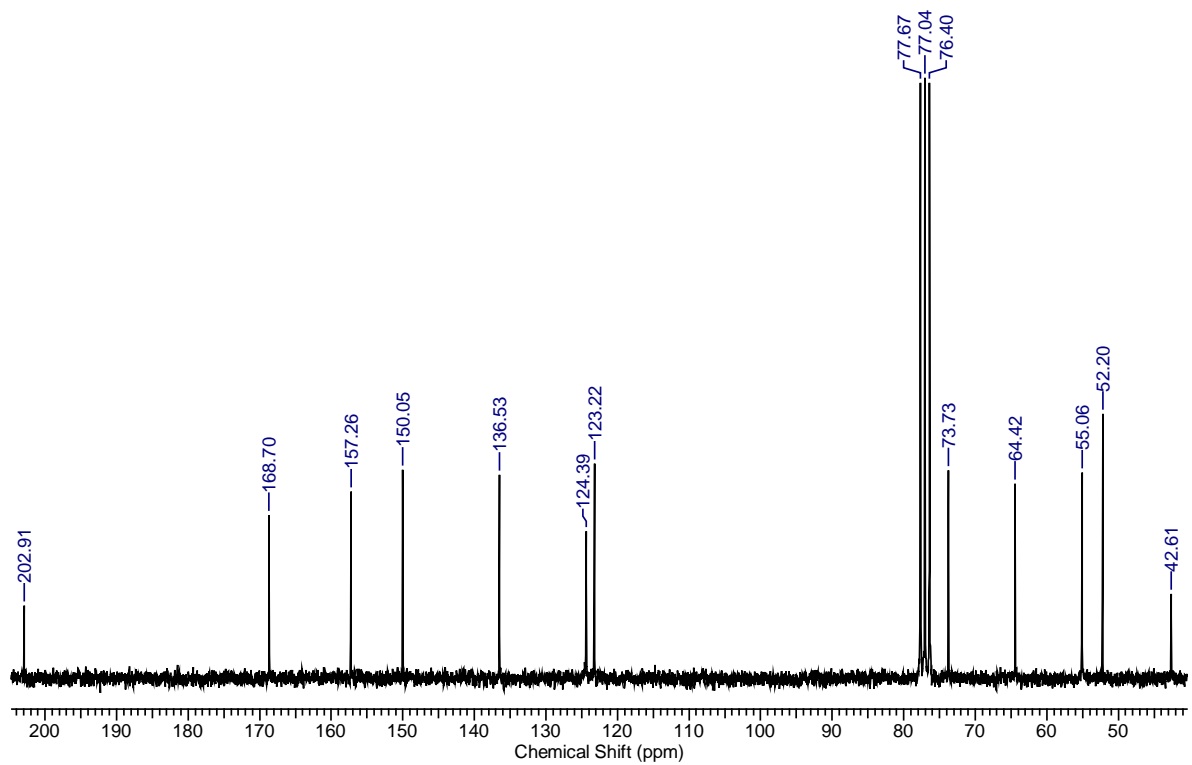
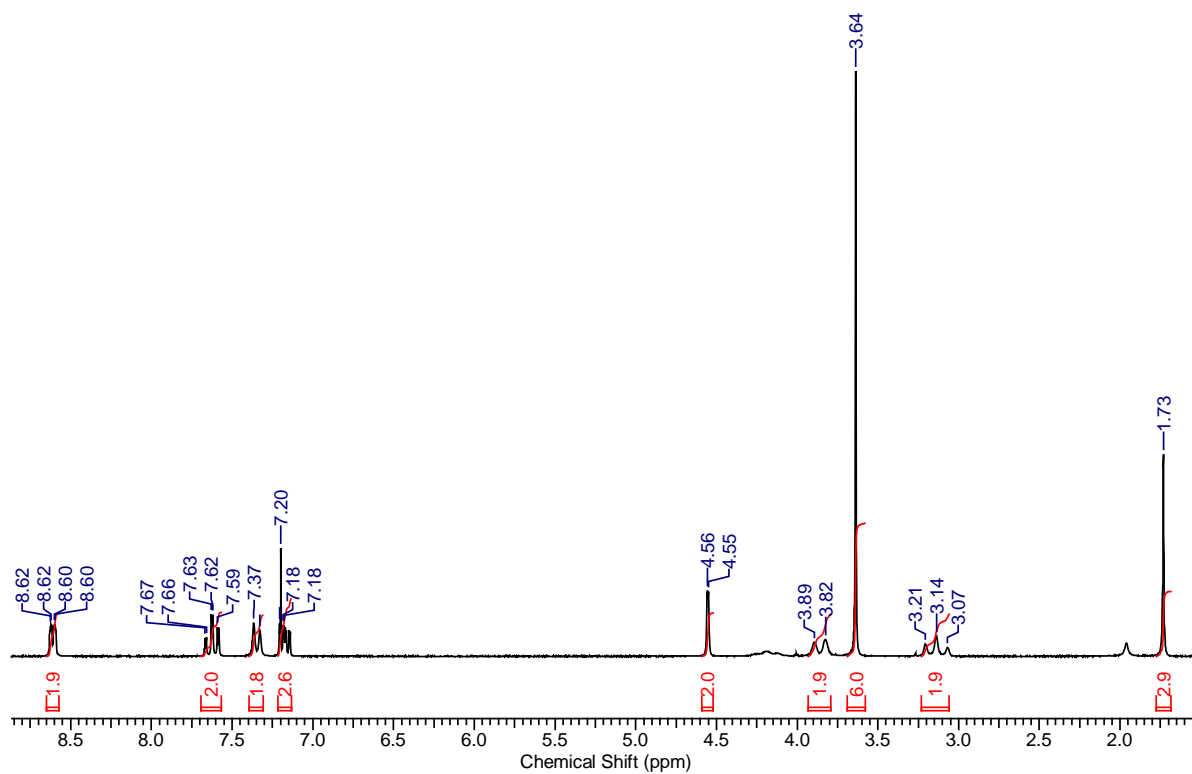


Figure S6: NMR Spectra of Dimethyl-(3-methyl-9-oxo-2,4-bis(2-pyridyl)-3,7-diazabicyclo[3.3.1]nonane)-1,5-dicarboxylate

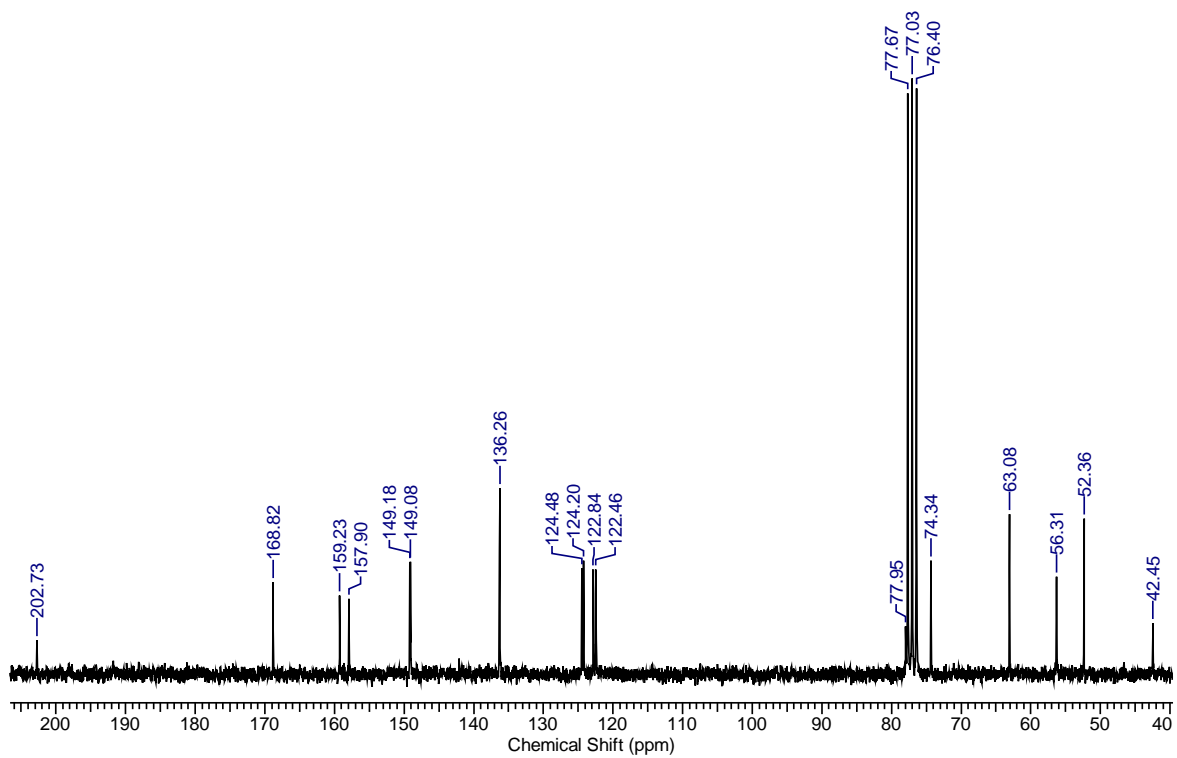
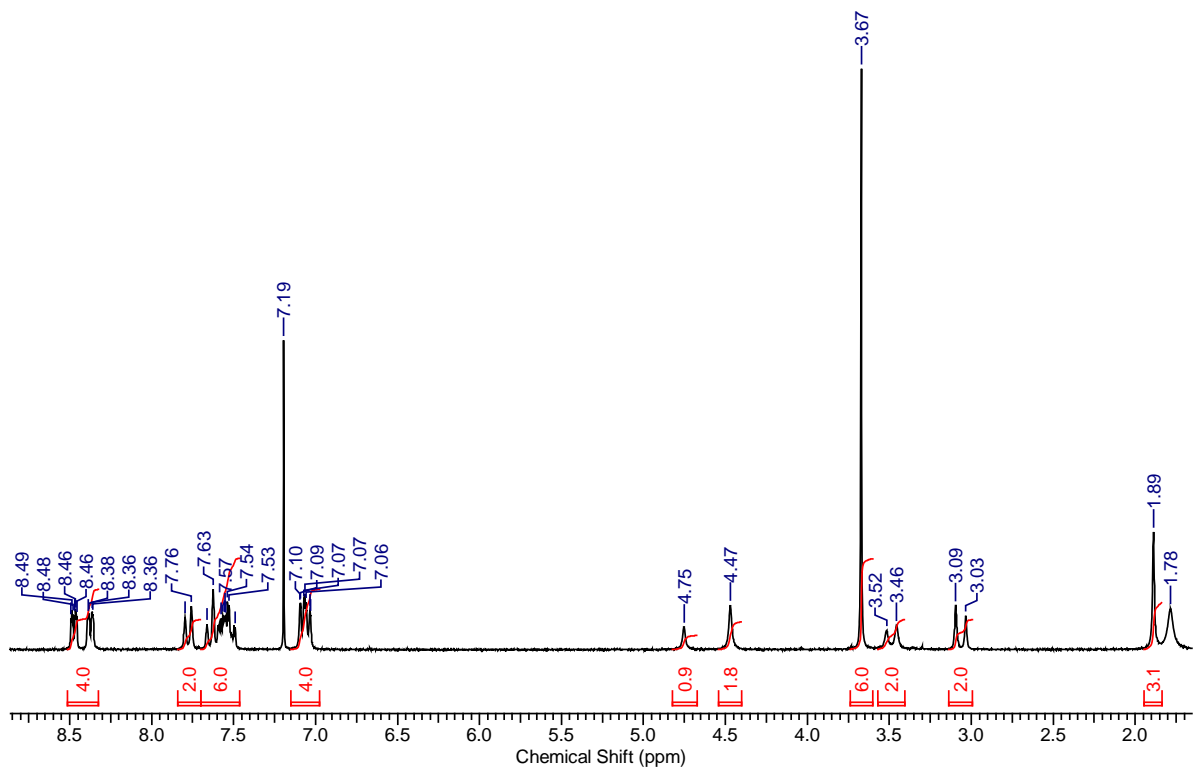


Figure S7: NMR Spectra of Dimethyl-(3-methyl-7-bis(2-pyridyl)methyl-9-oxo-2,4-bis(2-pyridyl)-3,7-diazabicyclo[3.3.1]nonane)-1,5-dicarboxylate

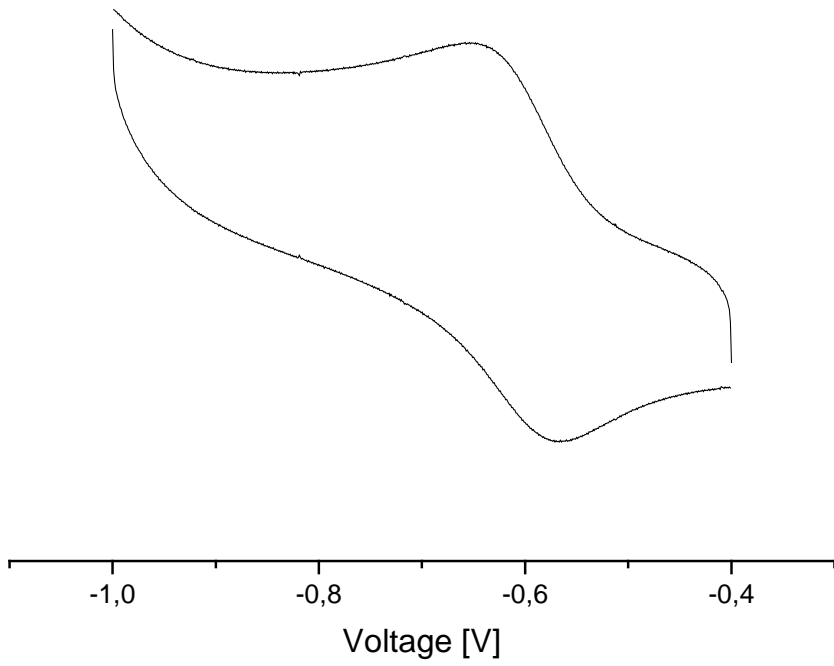


Figure S8: Cyclovoltammogramm of $[\text{Cu}(\text{L})](\text{BF}_4)_2$ in acetonitrile with 0.1M $(\text{Bu}_4\text{N})\text{PF}_6$ as supporting electrolyte vs. Ag/AgNO_3

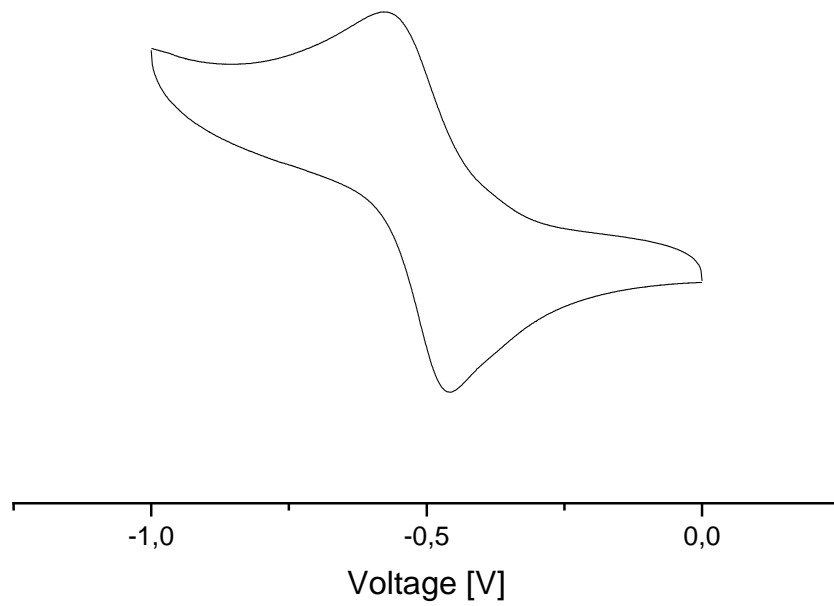


Figure S9: Cyclovoltammogramm of $[\text{Cu}(\text{L})](\text{BF}_4)_2$ in water with 3M NaCl as supporting electrolyte vs. Ag/AgCl

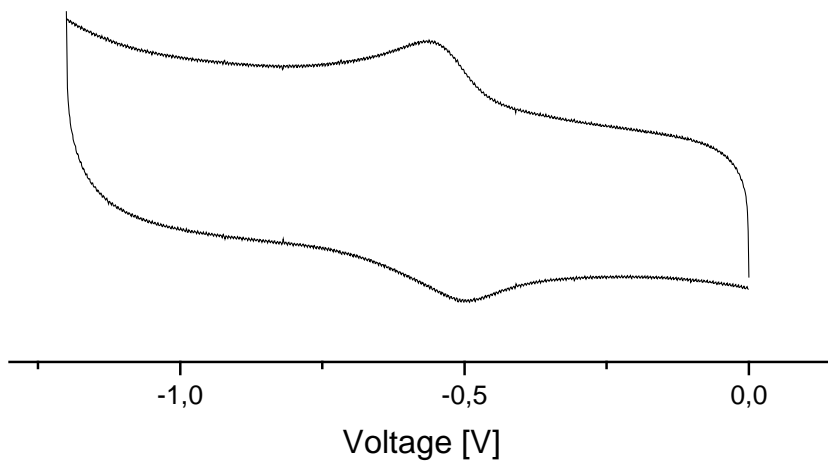


Figure S10: Cyclovoltammogramm of $[\text{Cu}(\text{L}^{\text{OH}})](\text{BF}_4)_2$ in acetonitrile with 0.1M $(\text{Bu}_4\text{N})\text{PF}_6$ as supporting electrolyte vs. Ag/AgNO_3

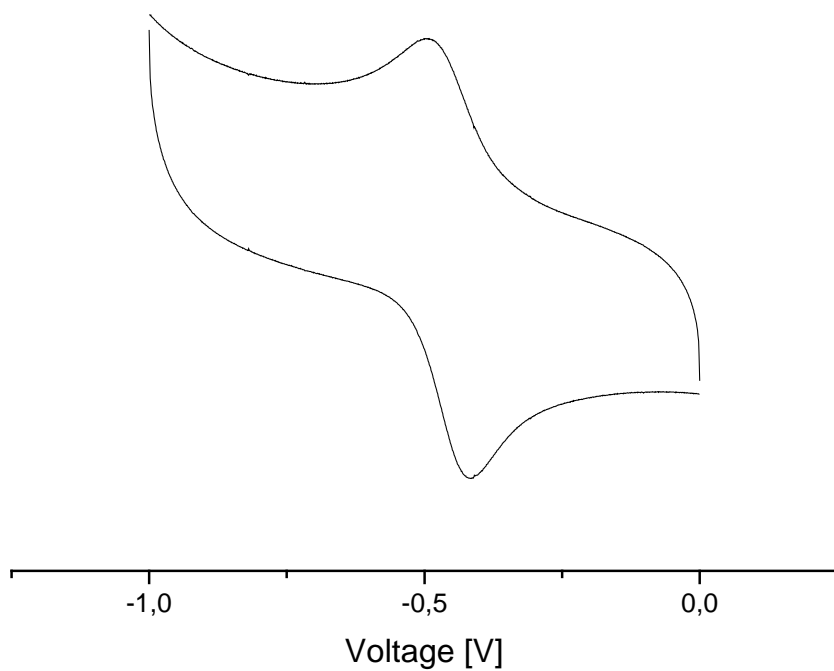


Figure S11: Cyclovoltammogramm of $[\text{Cu}(\text{L}^{\text{OH}})](\text{BF}_4)_2$ in water with 3M NaCl as supporting electrolyte vs. Ag/AgCl

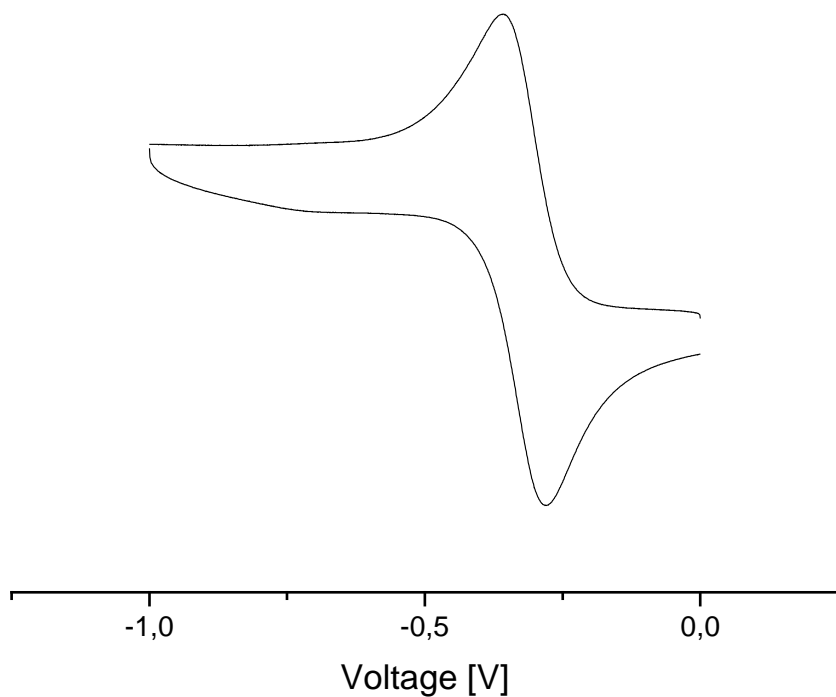


Figure S12: Cyclovoltammogramm of $[\text{Cu}(\text{L})](\text{ClO}_4)_2$ in acetonitrile with 0.1M $(\text{Bu}_4\text{N})\text{PF}_6$ as supporting electrolyte vs. Ag/AgNO_3

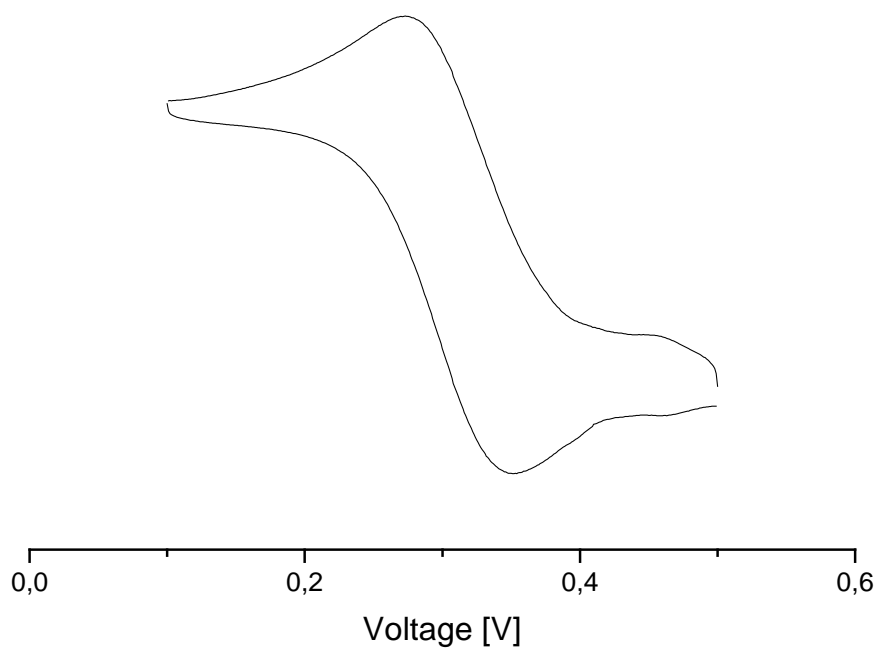


Figure S13: Cyclovoltammogramm of $[\text{Fe}(\text{L}^{\text{OH}})(\text{Cl})]\text{Cl}$ in acetonitrile with 0.1M $(\text{Bu}_4\text{N})\text{PF}_6$ as supporting electrolyte vs. Ag/AgNO_3

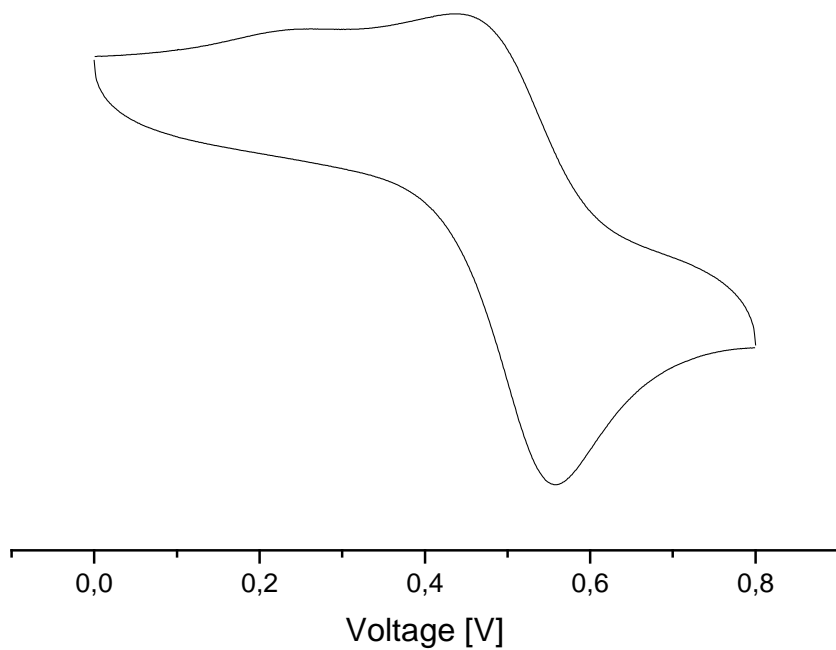


Figure S14: Cyclovoltammogramm of $[\text{Fe}(\text{L}^{\text{OH}})(\text{Cl})]\text{Cl}$ in water with 3M NaCl as supporting electrolyte vs. Ag/AgCl

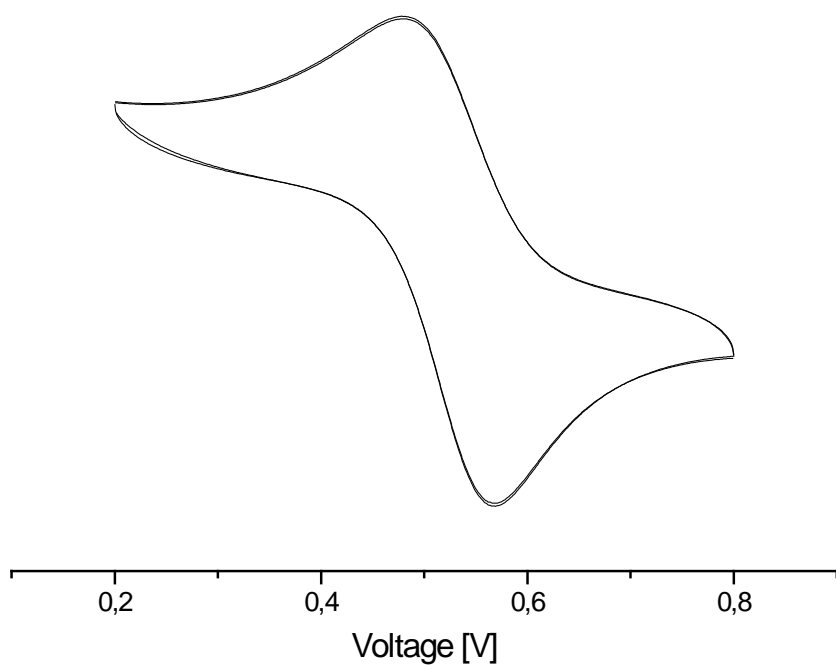


Figure S15: Cyclovoltammogramm of $[\text{Fe}(\text{L})(\text{OHMe})](\text{BF}_4)_2$ in water with 3M NaCl as supporting electrolyte vs. Ag/AgCl

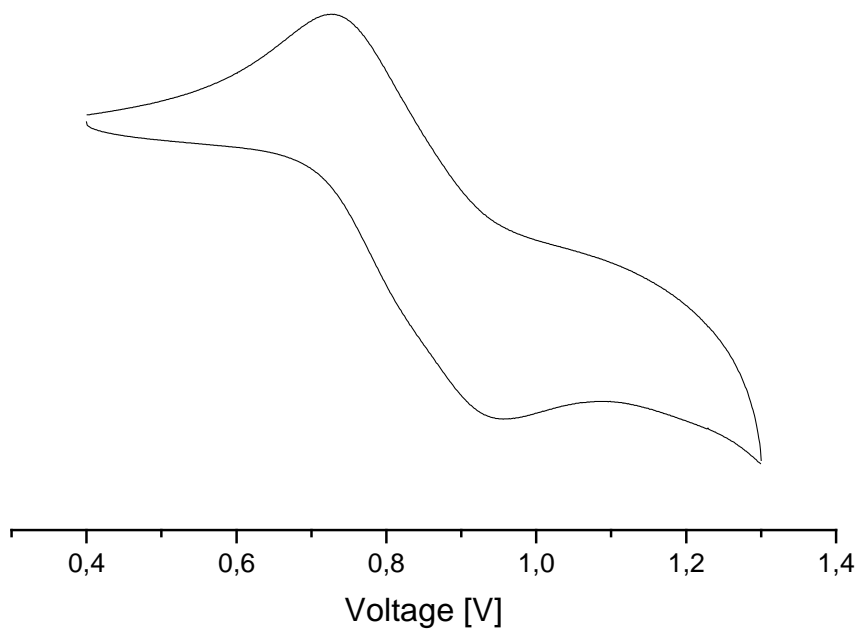


Figure S16: Cyclovoltammogramm of $[\text{Mn}(\text{L})(\text{Cl})]_2[\text{MnCl}_4]$ in acetonitrile with 0.1M $(\text{Bu}_4\text{N})\text{PF}_6$ as supporting electrolyte vs. Ag/AgNO_3